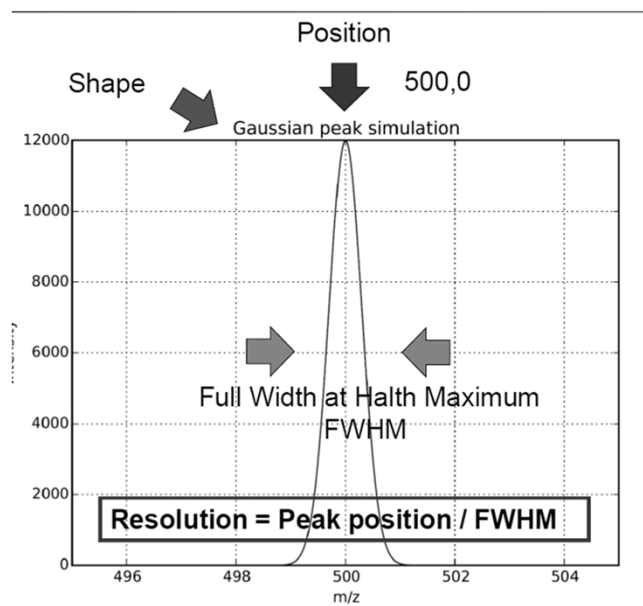


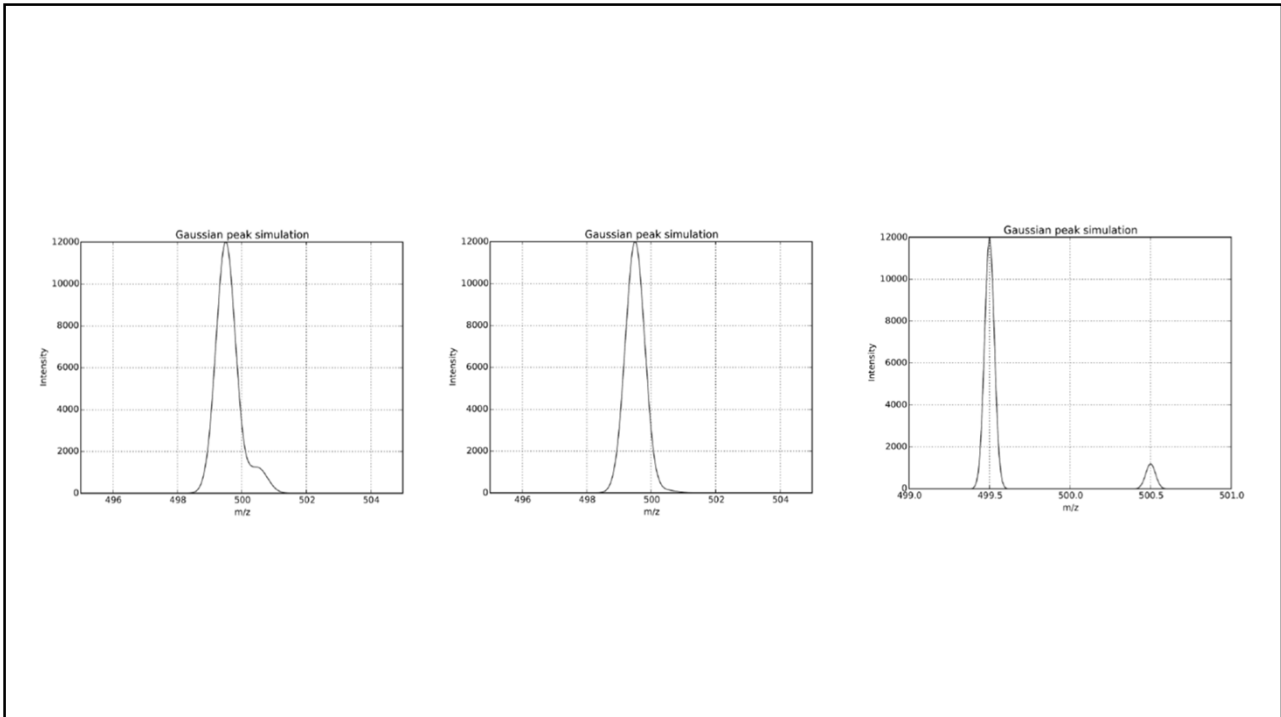
SPETTROMETRIA DI MASSA

Potere Risolutivo, Risoluzione e accuratezza di massa

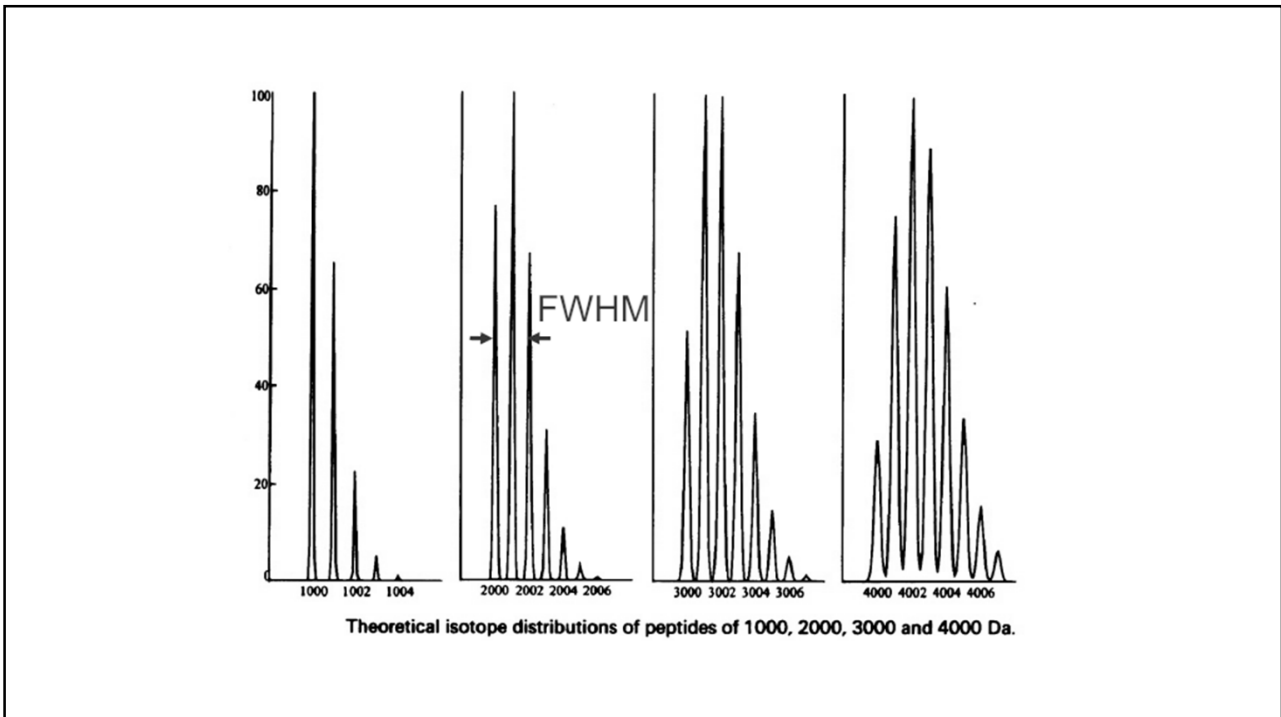
1



2



3



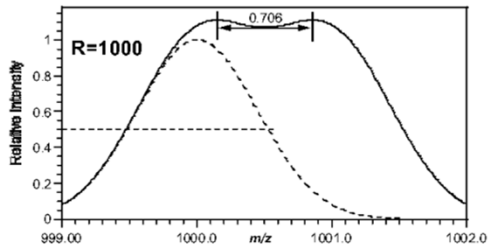
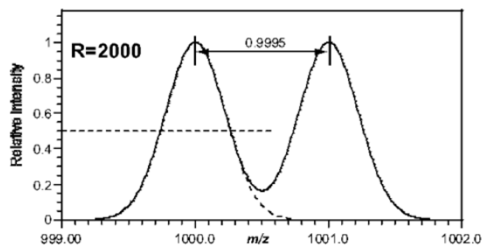
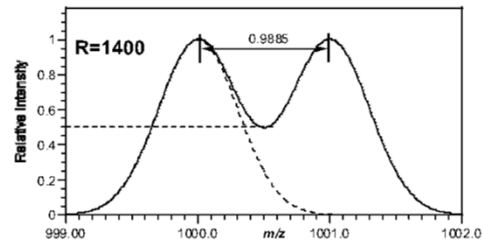
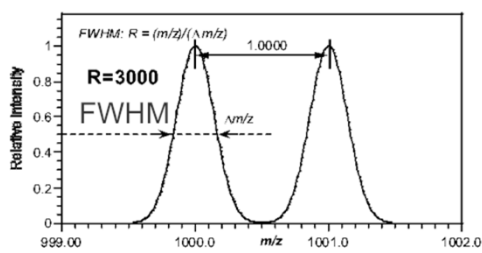
4

Isotope	Mass	Abundance	Chemical mass	Deviation from the whole number
¹ H	1.00782510	99.9852%	1.00794	+0.0079
² H (D)	2.01410222	0.0148%		
¹² C	12.0(0)	98.892%	12.011	+0.011
¹³ C	13.0033544	1.108%		
¹⁴ N	14.00307439	99.635%	14.00674	+0.007
¹⁵ N	15.0001077	0.365%		
¹⁶ O	15.99491502	99.759%	15.9994	-0.0006
¹⁷ O	16.9991329	0.037%		
¹⁸ O	17.99916002	0.204%		
³¹ P	30.9737647	100%	30.9737647	-0.0262
³² S	31.9720737	95.0%	32.066	+0.066
³³ S	32.9714619	0.76%		
³⁴ S	33.9678646	4.22%		
³⁶ S	35.967090	0.014%		

5

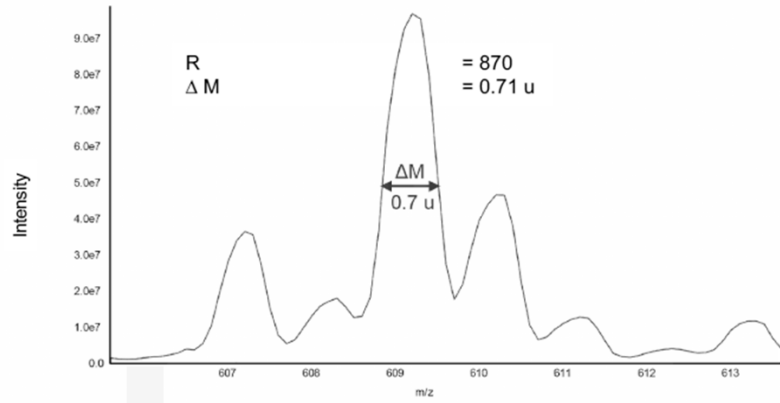
$$R = (m/z)_0 / \text{FWHM}(m/z)$$

FWHM: full width at half maximum



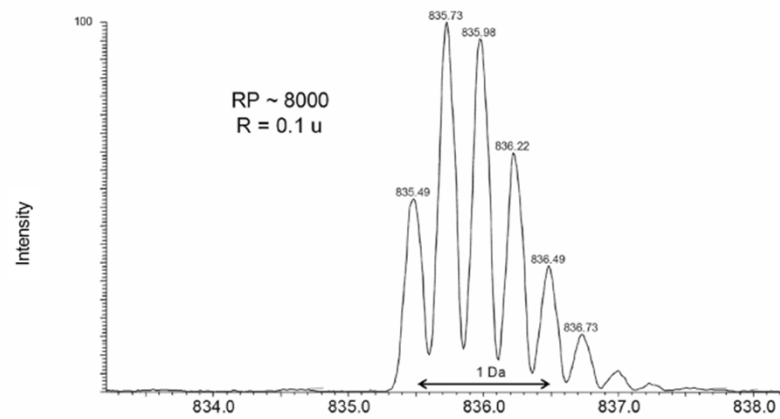
6

low resolution

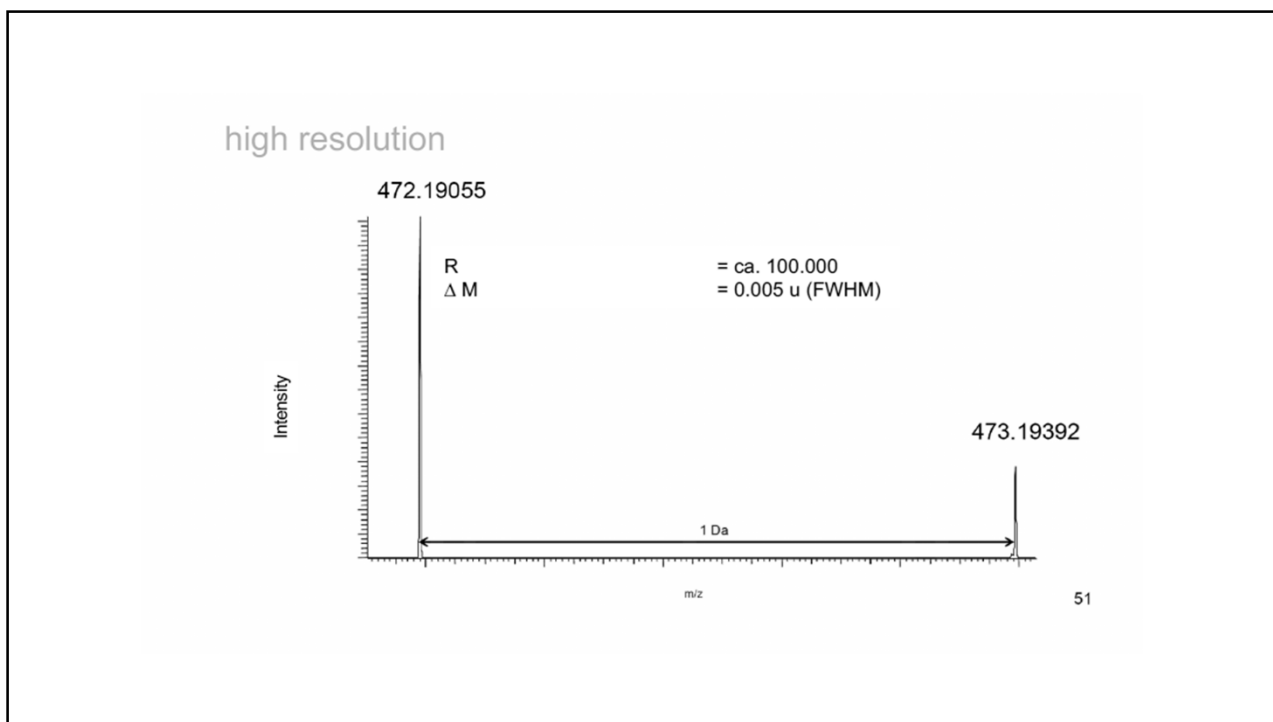


7

moderate resolution



8



9

Average Mass e.g. C=12.01115

Mass of an ion or molecule weighted for its *isotopic composition*.

Monoisotopic Mass (Exact Mass) e.g. C=12.000000

Exact mass of an ion or molecule calculated using the *mass of the most abundant isotope* of each element.

Nominal Mass e.g. C=12

Mass of a molecular ion or molecule calculated using the *isotope mass of the most abundant constituent* (ignoring mass defect) element isotope of each element rounded to the *nearest integer value* and multiplied by the number of atoms of each element (C=12, H=1, N=14, O=16,)

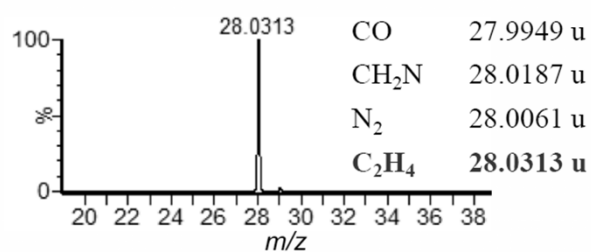
10

	mass	probability	¹ H	² H	¹² C	¹³ C	¹⁴ N	¹⁵ N	¹⁶ O	¹⁷ O	¹⁸ O	³² S	³³ S	³⁴ S	³⁶ S
1	5731.6075806688	0.1123023514	377	0	252	2	65	0	75	0	0	6	0	0	0
2	5732.6109355040	0.1028778936	377	0	251	3	65	0	75	0	0	6	0	0	0
3	5730.6042258336	0.0814037470	377	0	253	1	65	0	75	0	0	6	0	0	0
4	5733.6142903392	0.0704027660	377	0	250	4	65	0	75	0	0	6	0	0	0
5	5734.6176451744	0.0383896060	377	0	249	5	65	0	75	0	0	6	0	0	0
7	5733.6033765247	0.0301636876	377	0	252	2	65	0	75	0	0	5	0	1	0
6	5729.6008709984	0.0293871014	377	0	254	0	65	0	75	0	0	6	0	0	0
8	5734.6067313599	0.0276323390	377	0	251	3	65	0	75	0	0	5	0	1	0
9	5732.6046155640	0.0266824062	377	0	252	2	64	1	75	0	0	6	0	0	0

11

e.g. m/z 28 can have 4 different elemental compositions with different exact mass values.

CO	27.9949 u	CH ₂ N	28.0187 u
N ₂	28.0061 u	C ₂ H ₄	28.0313 u



12

- Mass error in millimass units (mmu)

$$[\text{measured mass (u)} - \text{theoretical mass (u)}] \times 1000$$
- Mass error in parts per million (ppm)

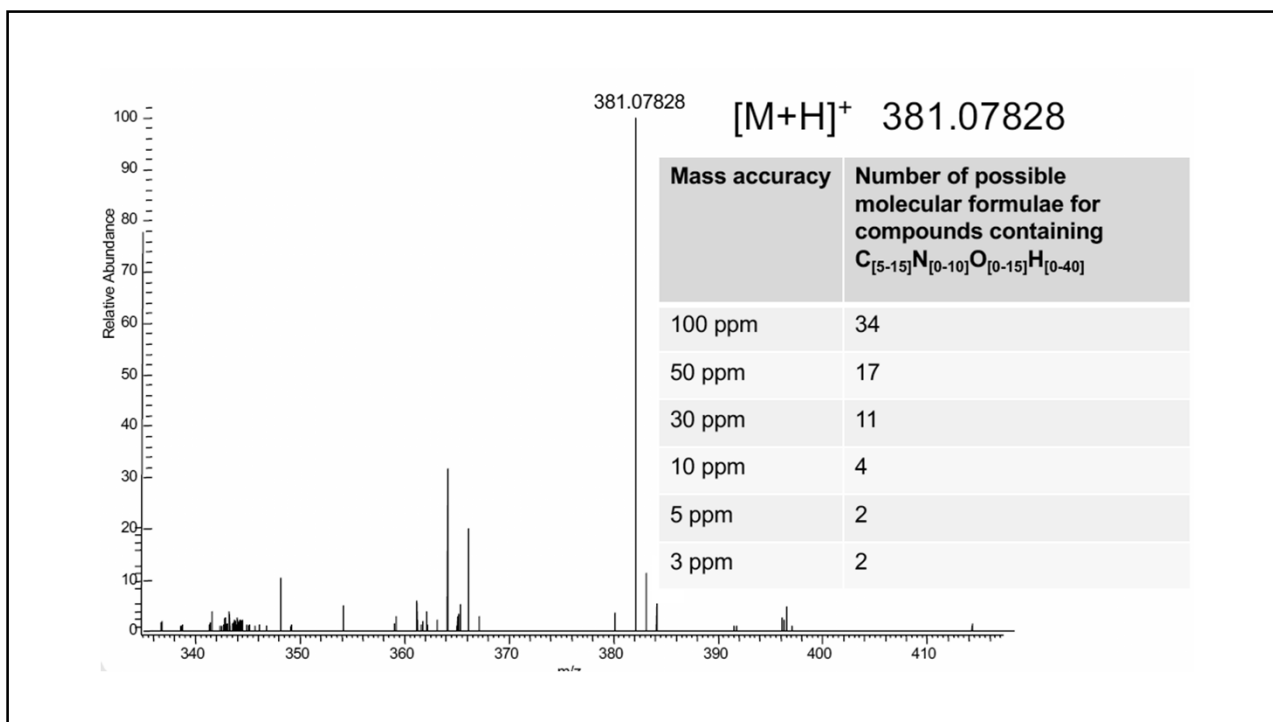
$$\frac{[\text{measured mass (u)} - \text{theoretical mass (u)}] \times 1000000}{\text{theoretical mass (u)}}$$

Measured Mass	Theoretical Mass	Mass Difference (u)	ppm error
200.0020	200.0000	0.002	$(0.002/200)1e^6 = 10 \text{ ppm}$
400.0020	400.0000	0.002	$(0.002/400)1e^6 = 5 \text{ ppm}$
800.0020	800.0000	0.002	$(0.002/800)1e^6 = 2.5 \text{ ppm}$
1000.0020	1000.0000	0.002	$(0.002/1000)1e^6 = 2 \text{ ppm}$
		Constant with mass	Varies with mass

13

Mass Analyzer	Mass Range (u)	Mass Resolution	Mass Accuracy (ppm)
Fourier Transform Ion Cyclotron Resonance (FT ICR)	30.000	1.000.000+	< 1 (@ 400 u)
Orbitrap	50.000	500.000	< 2 (@ 100-2000)
Magnetic Sector (BE)	20.000	100.000	< 10
Time-of-Flight (TOF, RTOF)	> 1.000.000	5.000-20.000	200; 5-10
Quadrupole (Q)	4.000	2.000	100
Iontrap (IT)	6.000	4.000	100

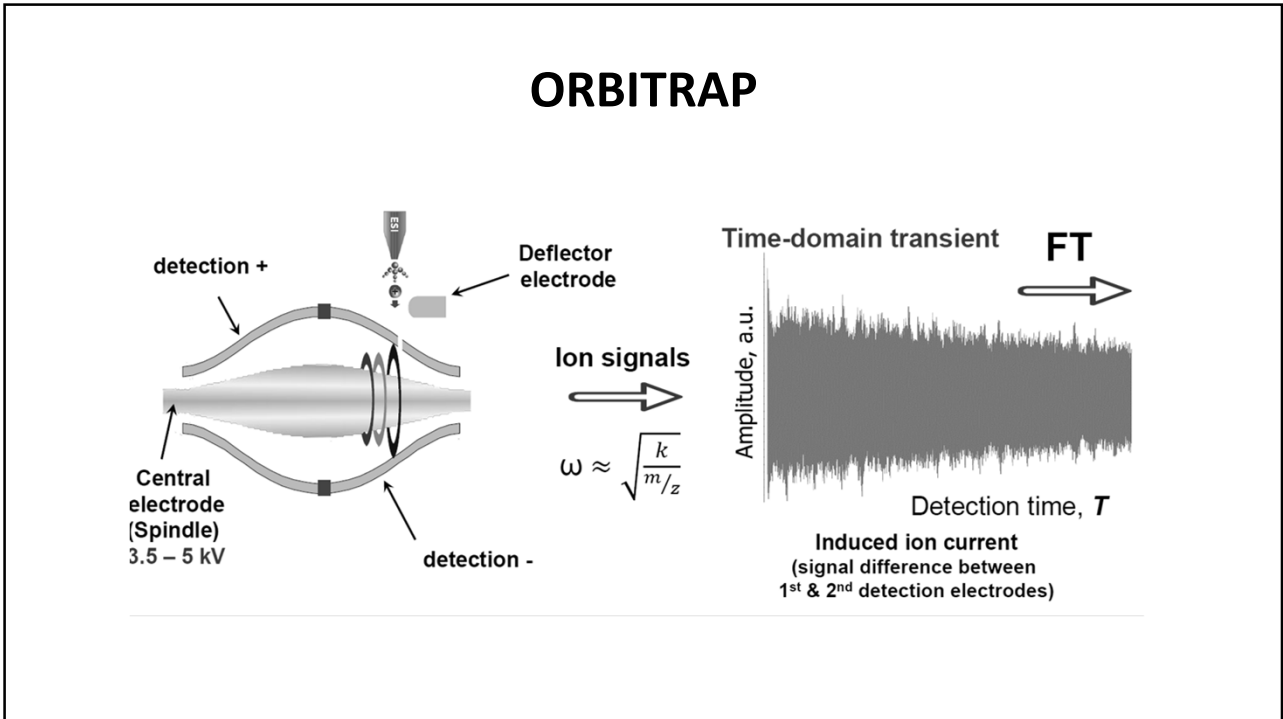
14



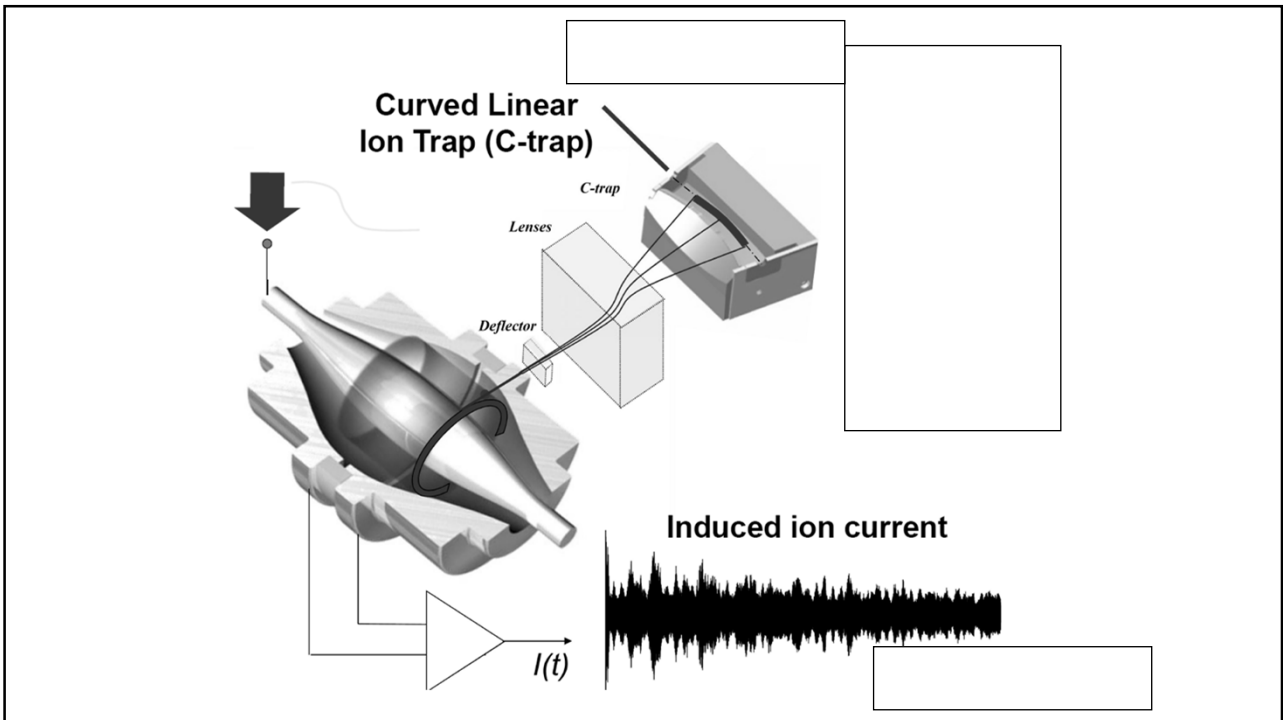
15

ANALIZZATORI DI MASSA AD ALTA RISOLUZIONE

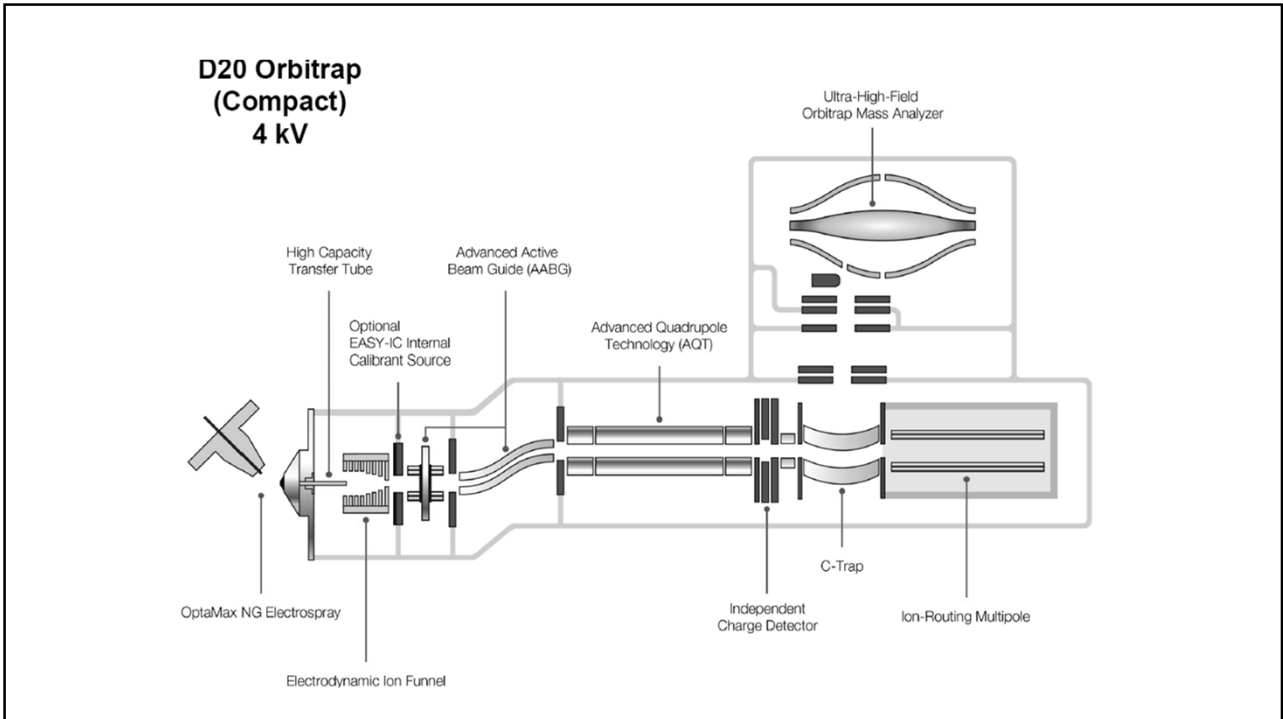
16



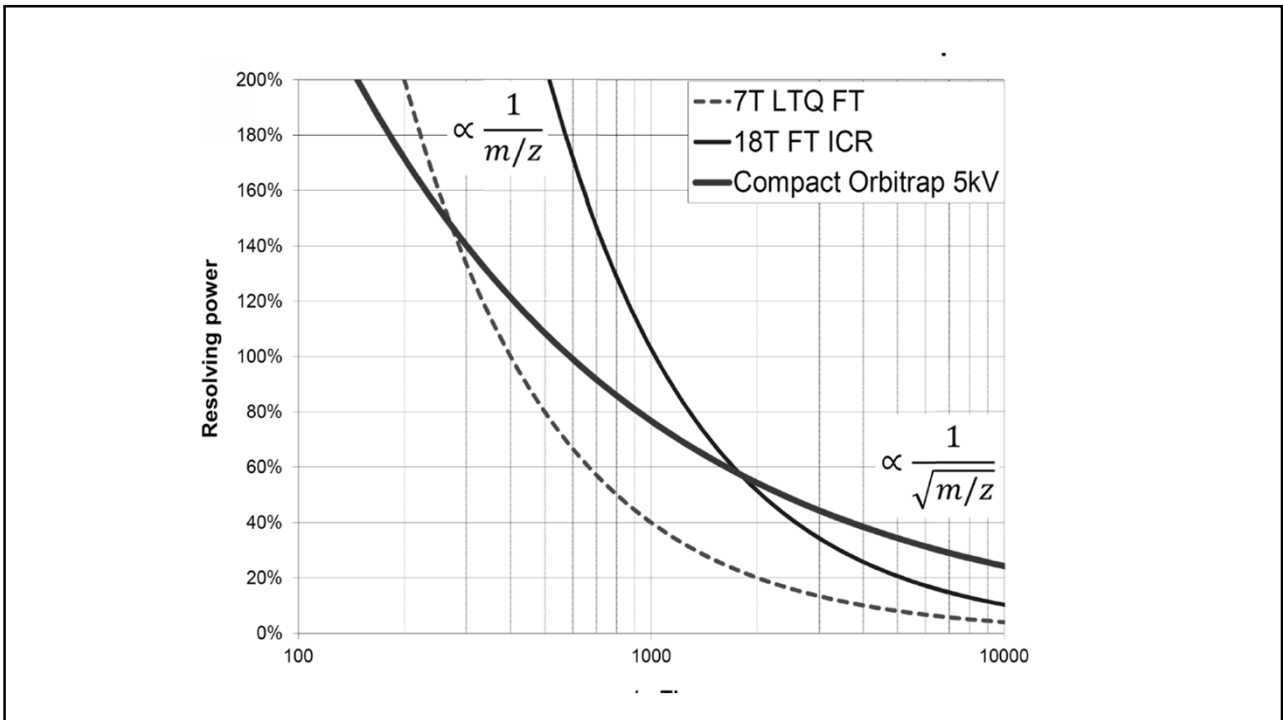
17



18



19



20

TIME OF FLIGHT

$$E_p = qU$$

$$E_k = \frac{1}{2}mv^2$$

$$E_p = E_k$$

$$qU = \frac{1}{2}mv^2 \quad v = \frac{d}{t}$$

$$t = k \sqrt{\frac{m}{q}}$$

The diagram shows a series of ions being accelerated from a source on the left, labeled '+ High voltage', towards a detector on the right, labeled 'Ground'. The distance between the source and the detector is marked as 'D'. A 'Laser' and 'Trigger' system is connected to the detector to measure the time of flight.

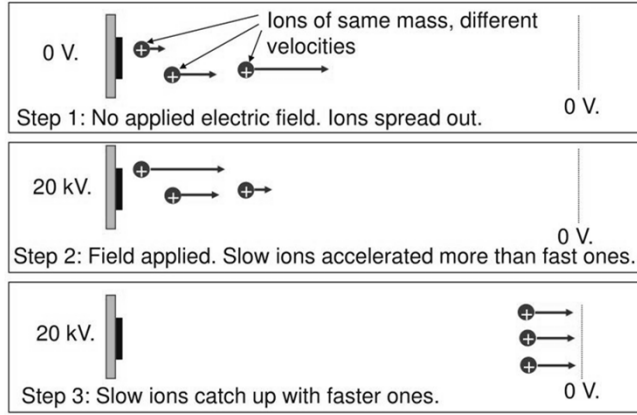
21

This diagram illustrates a microchannel plate detector setup. On the left, a 'laser head' is positioned above a 'microchannel plate detector'. The detector is connected to a '+V' terminal. An 'electromagnetic field' is shown around the detector. The ions travel through a 'reflectron' region, which is connected to '0V' and '+V' terminals. Another 'electromagnetic field' is shown around the reflectron.

22

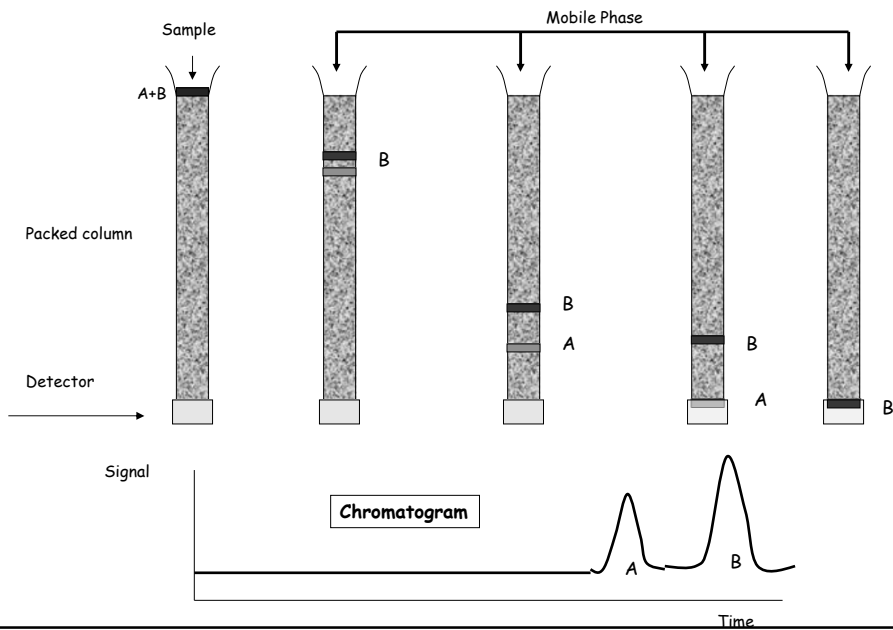
DELAYED EXTRACTION

Delayed Extraction (DE) improves performance

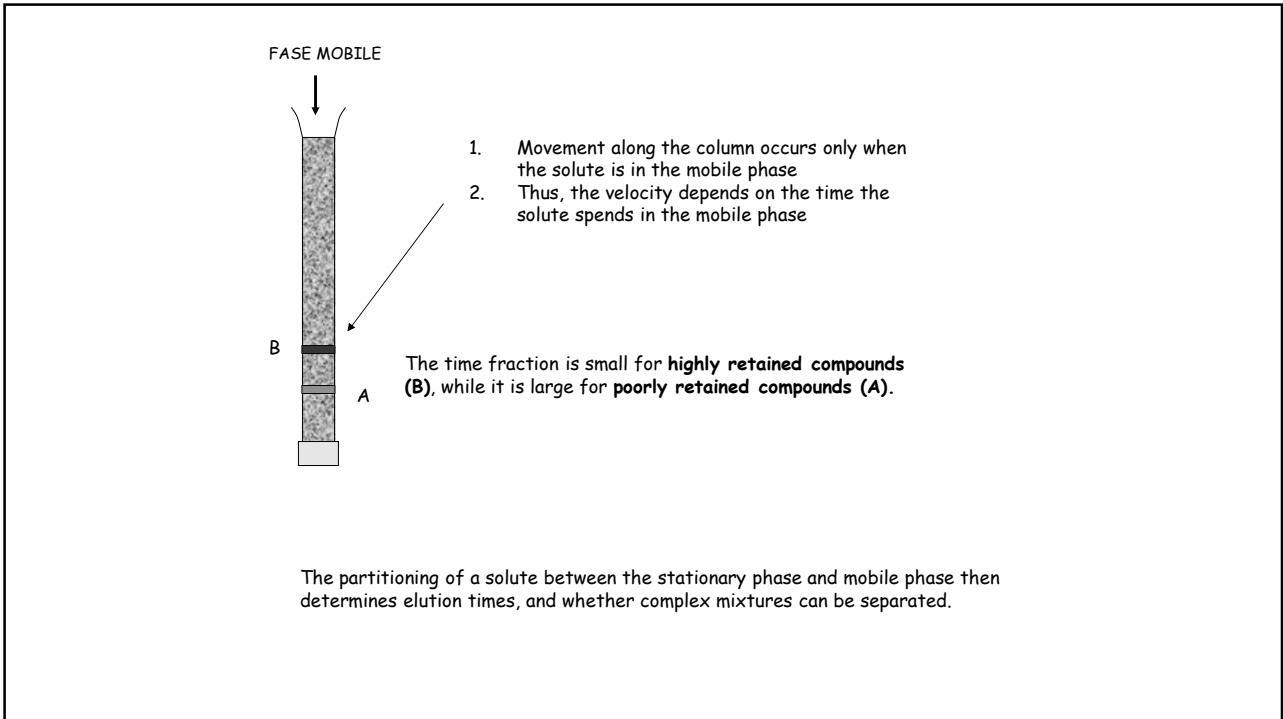


23

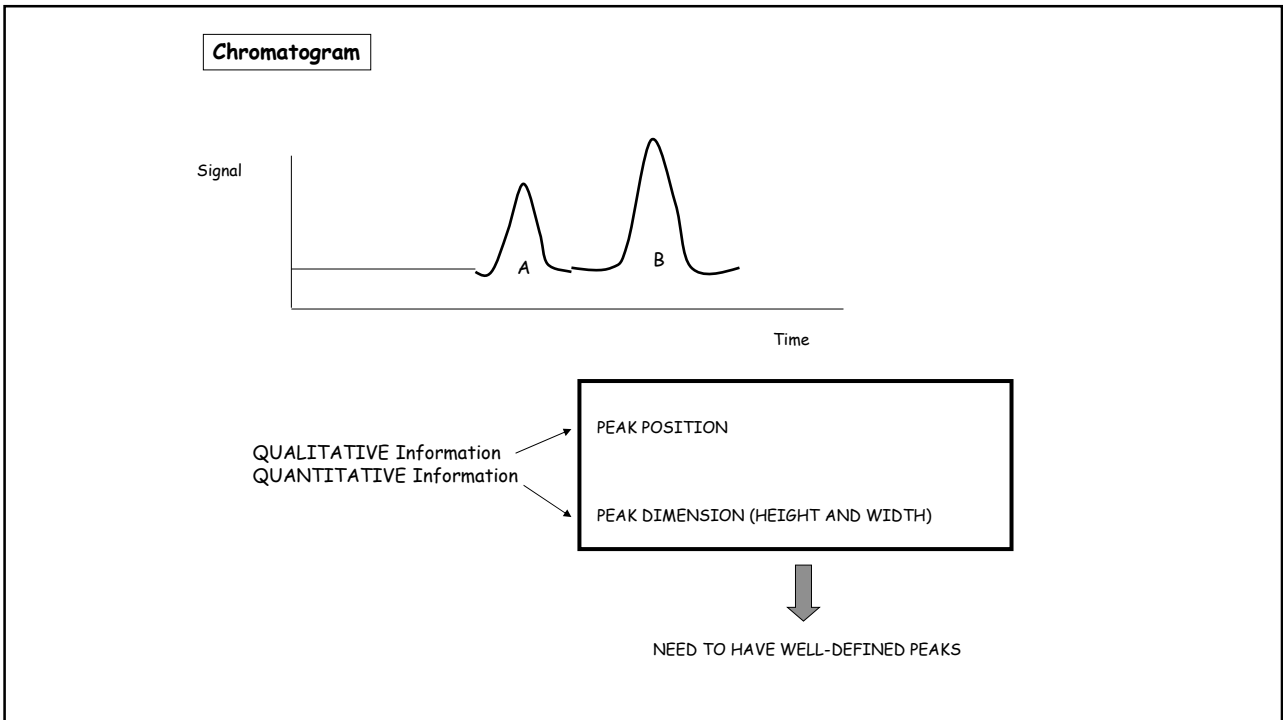
Column Chromatography



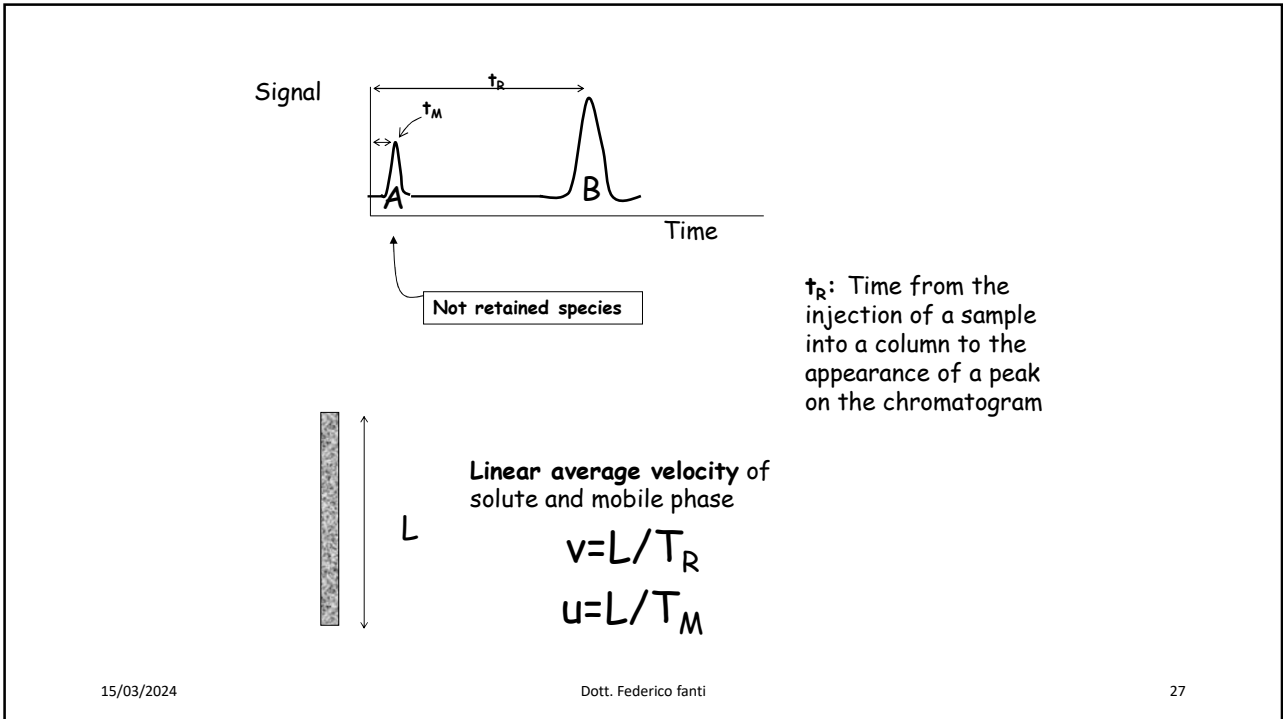
24



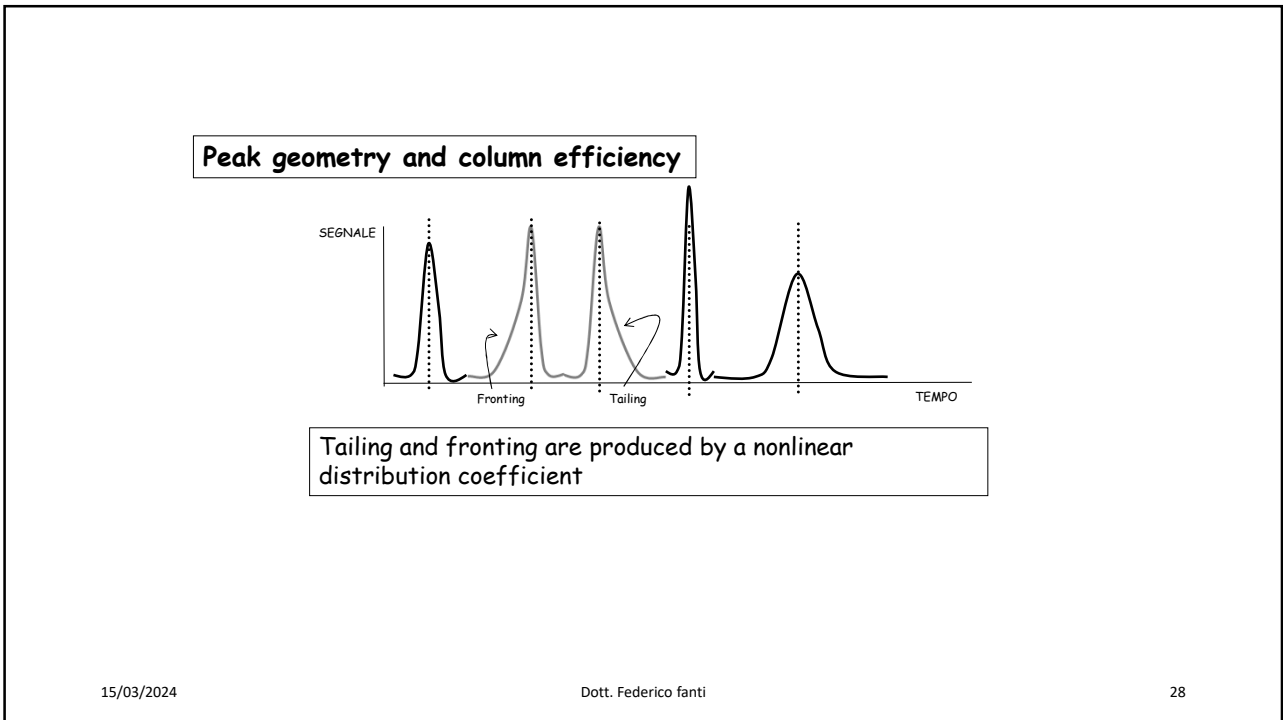
25



26



27

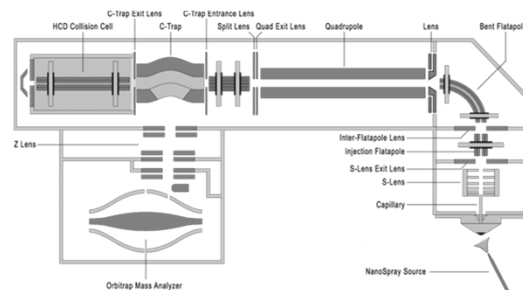
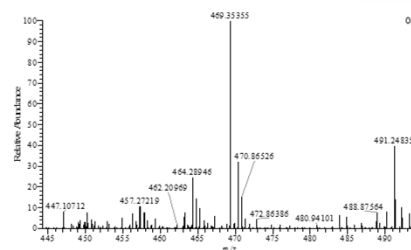
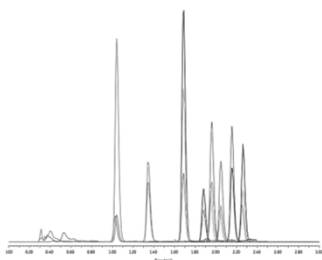


28

UHPLC-HRMS(/MS)

Identification by:

- ✓ Retention Time
- ✓ Mass Spectrum
 - Accurate Mass
 - Parent Ion
 - Fragment Ions
 - Fragment intensity ratio

**Acquisition Mode:**

- ✓ Full Scan
- ✓ HRMS/MS
- ✓ Data-Dependent Scan (FS-ddA)
- ✓ Selected Ion Monitoring

29

Omics sciences

The omics sciences study pools of biological molecules (e.g., ions, nucleic acids, proteins, enzymes) with various functions within living organisms. These functions are related to the abilities, inherent in such molecules, to be able to transform (translation process) their structures and chemical and/or electrostatic bonds into energetic/biochemical processes aimed at creating other structures or interacting with other structures, with the ultimate goal of modifying/creating structures or functions different from the original ones.

The omics sciences thus have the primary goal of analyzing as a whole:

1. the genes contained in DNA (genomics) and their multiple functions (functional genomics);
2. the product of DNA transcription: the RNA (transcriptomics);
3. the proteins encoded by DNA through RNA (proteomics);
4. the molecules that interact within an organism (metabolites: metabolomics).

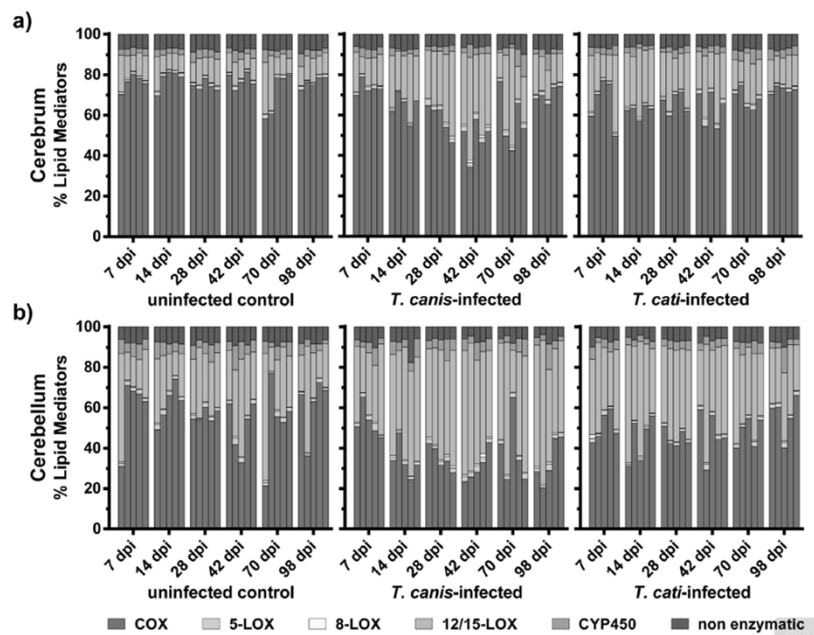
30

RESEARCH ARTICLE

Multiplex profiling of inflammation-related bioactive lipid mediators in *Toxocara canis*- and *Toxocara cati*-induced neurotoxocarosis

Patrick Waindok¹, Elisabeth Janecek-Erfurth^{1,2a}, Dimitri Lindenwald^{1,2b}, Esther Wilk², Klaus Schughart^{2,3}, Robert Geffers⁴, Laurence Balas⁵, Thierry Durand⁵, Katharina Maria Rund^{6,7}, Nils Heige Schebb^{6,7}, Christina Strube^{1*}

31



32

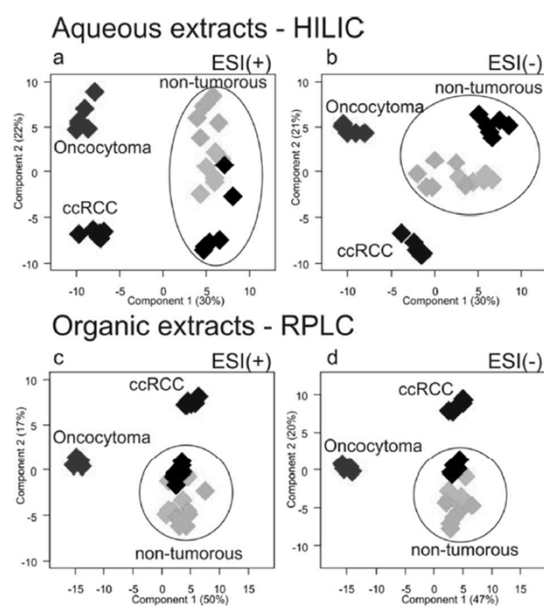
Comprehensive metabolomic and lipidomic profiling of human kidney tissue: a platform comparison

Patrick Leuthold, Elke Schaeffeler, Stefan Winter, Florian Büttner, Ute Hofmann,
Thomas E Mürdter, Steffen Rausch, Denise Sonntag, Judith Wahrheit, Falko
Fend, Jörg Hennenlotter, Jens Bedke, Matthias Schwab, and Mathias Haag

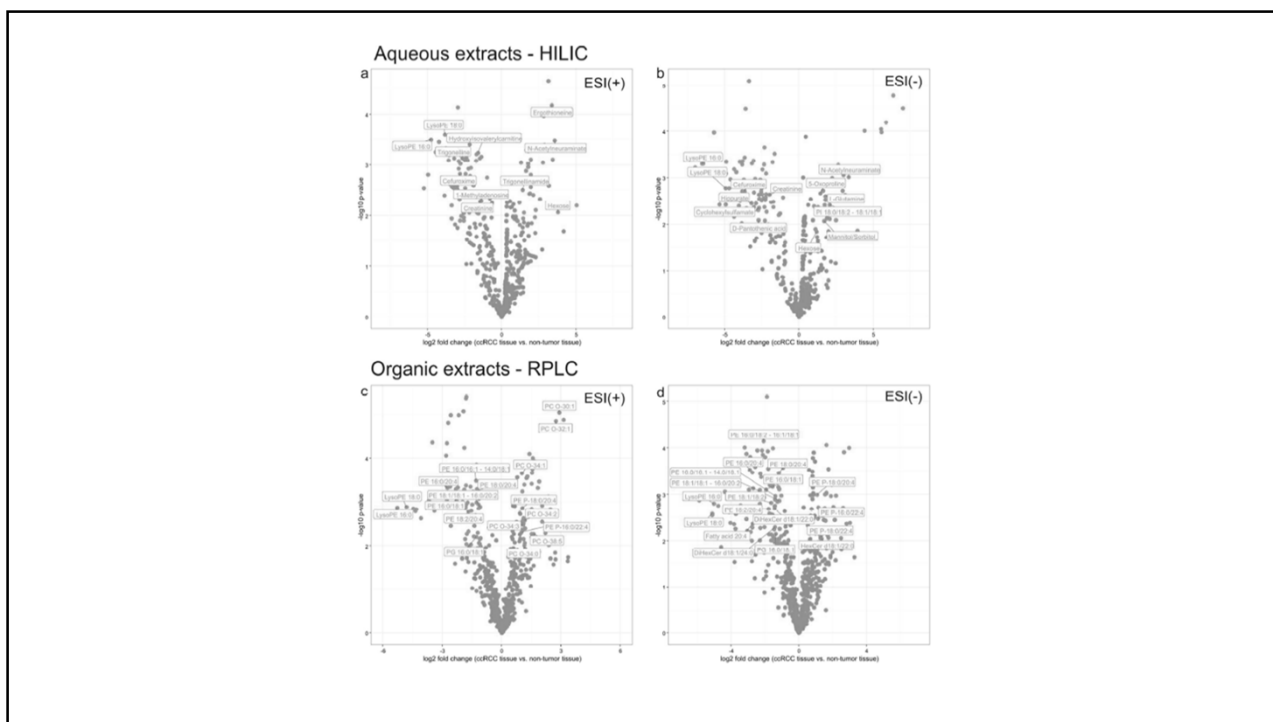
J. Proteome Res., Just Accepted Manuscript • DOI: 10.1021/acs.jproteome.6b00875 • Publication Date (Web): 19 Dec 2016

Downloaded from <http://pubs.acs.org> on December 20, 2016

35



36



37

**SCIENTIFIC
REPORTS**
nature research

OPEN **LC-HRMS based approach to
identify novel sphingolipid
biomarkers in breast cancer
patients**

Priyanka Bhadwal¹, Divya Dahiya², Dhananjay Shinde³, Kim Vaiphei⁴,
Raviswamy G. H. Math⁵, Vinay Randhawa¹ & Navneet Agnihotri^{1*}

38

Characteristics	
Number of patients	31
Age (Years)	
Median (Range)	50 (32-76)
≤50	16
>50	15
Tumor Type	
Ductal carcinoma <i>in situ</i> (DCIS)	1
Invasive ductal carcinoma	28
Metastatic carcinoma	2
Tumor subtypes	
ER+/PR+	20
ER+/PR-	6
Her2neu+	4
Triple Negative	1
Nodal Status	
Positive	15
Negative	16
Ki67 (%)	
≤30 (%)	25
>30 (%)	6
TNM Staging	
IA	8
IIA	10
IIB	3
IIIA	5
IIIC	3
IV	2

Table 1. Clinicopathological characteristics of patients with breast cancer.

Class	Fatty acid	Retention Time(min)	Molecular Formula	Observed Mass	Error (ppm)	Calculated Mass	MS/MS fragments (m/z)
Cer	(d18:1/12:0) (IS)	3.0	C30 H58 O3 N1	526.4484292	-1.76	481.4495	283,270,88
	(d18:1/16:0)	3.0	C35 H68 O5 N1	582.5112221	-1.93	537.5121	311,298,88
	(d18:1/18:1)	2.9	C37 H70 O5 N1	608.5272988	-2.63	563.5277	102
	(d18:1/23:2)	2.9	C43 H80 O5 N1	690.6053293	-1.49	631.5903	390,347,235
	(d18:1/24:1)	2.9	C43 H82 O5 N1	692.6212052	-2.32	647.6216	546,390,237
	(d18:2/16:0)	3.0	C35 H66 O5 N1	580.4956225	-2.11	535.4964	256,104
	(d18:2/23:0)	2.9	C42 H80 O5 N1	678.6055060	-2.22	633.6060	102
	(d18:2/24:1)	2.9	C43 H80 O5 N1	690.6053805	-2.00	645.6060	316,168
	(d18:1/25:0) (IS)	2.9	C44 H86 O5 N1	708.6525276	-2.30	663.6529	495,439,102
	(d18:0/16:0)	3.0	C34 H70 O3 N1	584.5269029	-2.06	539.5277	280,255,237
DHCer	(d18:0/18:1)	2.9	C37 H72 O5 N1	610.5425634	-1.91	565.5434	102
	(d18:0/21:2)	2.9	C41 H78 O5 N1	664.5900060	-1.97	605.5747	618,364
	(d18:1/12:0) (IS)	8.0	C42 H80 O13 N1	806.5628915	0.26	805.5551	190,146,102
SM	(d18:1/21:1)	7.2	C46 H90 O8 N2 P1	829.646159	-2.36	770.6302	392,168,78
	(d18:2/22:0)	7.2	C45 H90 O6 N2 P1	785.6525117	1.64	784.6458	184,86
	(d18:1/12:0) (IS)	7.3	C35 H72 O6 N2 P1	647.5118463	1.78	646.5050	184,102
DHSM	(d18:0/18:1)	7.2	C41 H84 O6 N2 P1	731.6055663	1.82	730.5989	184,102
	(d18:0/24:2)	7.1	C47 H94 O6 N2 P1	813.6838264	1.57	812.6771	184,86
	(d18:0/22:1)	7.2	C45 H91 O6 N2 P1	787.6683	1.27	786.6615	102

Table 3. Identification of sphingolipids in breast tissue using UHPLC in "Organic Phase Extract". IS- Internal Standard; CerP- Ceramide 1-Phosphate; So- Sphingosine/Sphinganine; S1P- Sphingosine 1-Phosphate; Cer- Ceramide; DHCer- Dihydro Ceramide; LacCer- Lactosyl Ceramide; SM- Sphingomyelin; DHSM- DihydroSphingomyelin.

39

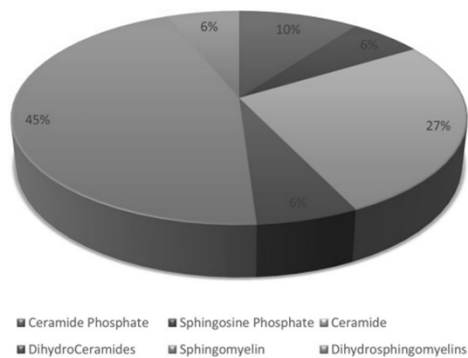
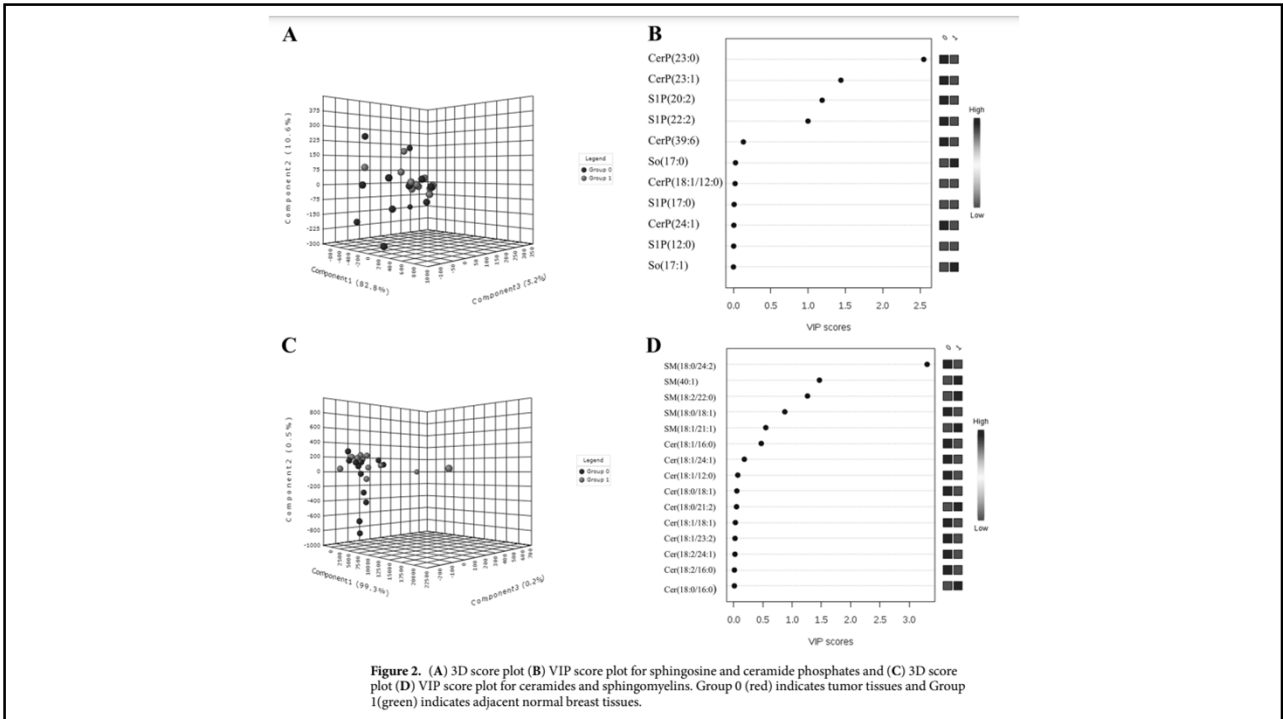
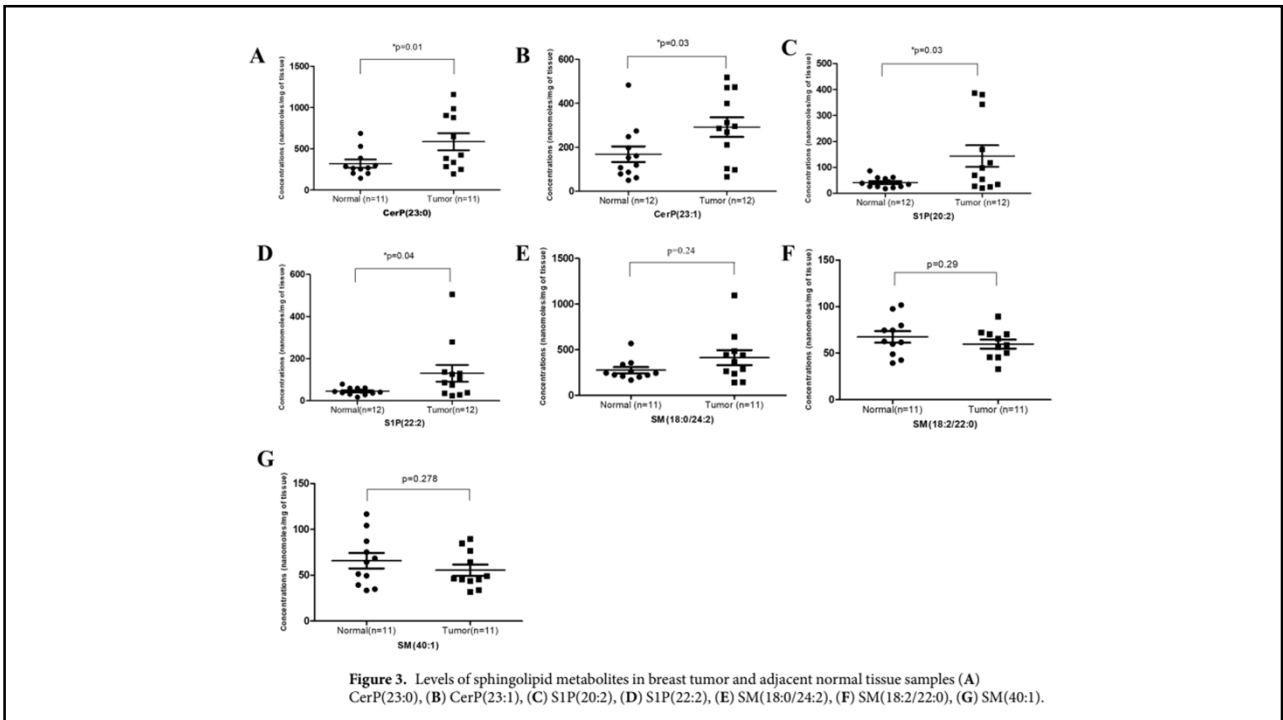


Figure 1. Pie chart representing the abundance of sphingolipid metabolites in breast tissue.

40



41



42

